

See discussions, stats, and author profiles for this publication at: <https://www.researchgate.net/publication/50998280>

Solubility of Acetic Acid and Trifluoroacetic Acid in Low-Temperature (207–245 K) Sulfuric Acid Solutions: Implications for the Upper Troposphere and Lower Stratosphere

ARTICLE in THE JOURNAL OF PHYSICAL CHEMISTRY A · APRIL 2011

Impact Factor: 2.69 · DOI: 10.1021/jp200118g · Source: PubMed

READS

21

5 AUTHORS, INCLUDING:



M. P. Sulbaek Andersen

California State University, Northridge

61 PUBLICATIONS 1,808 CITATIONS

SEE PROFILE



Jessica Axson

University of Michigan

21 PUBLICATIONS 99 CITATIONS

SEE PROFILE



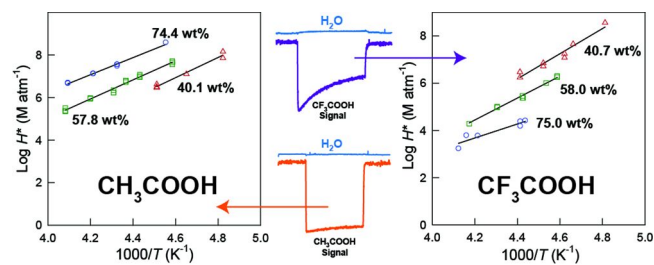
Ole John Nielsen

University of Copenhagen

263 PUBLICATIONS 4,915 CITATIONS

SEE PROFILE

The following graphic will be used for the TOC:



Solubility of Acetic Acid and Trifluoroacetic Acid in Low-Temperature (207–245 K) Sulfuric Acid Solutions: Implications for the Upper Troposphere and Lower Stratosphere

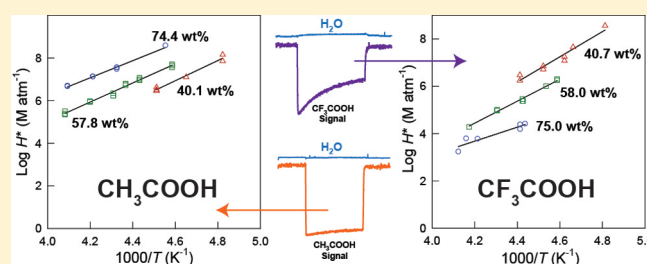
Mads P. Sulbaek Andersen,^{*,†,‡,||} Jessica L. Axson,^{§,⊥} Rebecca R. H. Michelsen,[§] Ole John Nielsen,[†] and Laura T. Iraci^{*,‡}

[†]Department of Chemistry, University of Copenhagen, Universitetsparken 5, DK-2100 Copenhagen, Denmark

[‡]Atmospheric Science Branch, NASA Ames Research Center, Moffett Field, California 94035, United States

[§]Department of Chemistry, Randolph-Macon College, Ashland, Virginia 23005-5505, United States

ABSTRACT: The solubility of gas-phase acetic acid (CH_3COOH , HAc) and trifluoroacetic acid (CF_3COOH , TFA) in aqueous sulfuric acid solutions was measured in a Knudsen cell reactor over ranges of temperature (207–245 K) and acid composition (40–75 wt %, H_2SO_4). For both HAc and TFA, the effective Henry's law coefficient, H^* , is inversely dependent on temperature. Measured values of H^* for TFA range from $1.7 \times 10^3 \text{ M atm}^{-1}$ in 75.0 wt % H_2SO_4 at 242.5 K to $3.6 \times 10^8 \text{ M atm}^{-1}$ in 40.7 wt % H_2SO_4 at 207.8 K. Measured values of H^* for HAc range from $2.2 \times 10^3 \text{ M atm}^{-1}$ in 57.8 wt % H_2SO_4 at 245.0 K to $3.8 \times 10^8 \text{ M atm}^{-1}$ in 74.4 wt % H_2SO_4 at 219.6 K. The solubility of HAc increases with increasing H_2SO_4 concentration and is higher in strong sulfuric acid than in water. In contrast, the solubility of TFA decreases with increasing sulfuric acid concentration. The equilibrium concentration of HAc in UT/LS aerosol particles is estimated from our measurements and is found to be up to several orders of magnitude higher than those determined for common alcohols and small carbonyl compounds. On the basis of our measured solubility, we determine that HAc in the upper troposphere undergoes aerosol partitioning, though the role of H_2SO_4 aerosol particles as a sink for HAc in the upper troposphere and lower stratosphere will only be discernible under high atmospheric sulfate perturbations.



1. INTRODUCTION

Submicrometer sulfate particles constitute the principal mode of aerosols in the upper troposphere (UT) and lower stratosphere (LS). It is well established that the composition and size of these aerosols and reaction in or on their surfaces can significantly perturb the chemistry of the stratosphere.¹ In-situ measurements in certain regimes of the UT suggest that oxygenated volatile organic compounds (OVOCs), including small carboxylic acids, can contribute more mass to the aerosols than sulfate.² Uptake of OVOCs into aerosol particles may perturb the gas-phase concentrations, the composition of the aerosol particles, and, potentially, the cloud nucleation properties of those particles.³ Furthermore, uptake and/or reaction of OVOCs can also result in a substantial increase in the global radiative forcing of the sulfate aerosols.⁴

Small carboxylic acids are ubiquitous in the atmosphere, in both the gaseous and the particulate phases, with acetic acid, CH_3COOH (HAc), being one of the most abundant.⁵ Significant direct emissions (up to 48 Tg/year) of HAc have been established with biomass burning emissions likely being the major direct emission source.⁶ Still, photochemical oxidation of volatile organic compounds (VOCs) is thought to be the overall dominant source (38–75 Tg/year) of atmospheric HAc.^{7,8} Photolysis does not play a role in the destruction of atmospheric

HAc. Loss via dry and wet deposition is understood as the dominant fate of HAc in the troposphere, and estimates regarding tropospheric residence time span from days to weeks.⁹ Tropical and extra-tropical deep convection can loft boundary layer air rapidly and inject VOCs into the upper troposphere and occasionally into the stratosphere,^{10–12} and it is possible that ventilation of HAc from the lower troposphere to the UT/LS can occur during this rapid convection. Even in more temperate regions, mixing ratios of OVOCs at 10 km have been observed to double when convection over polluted areas takes place.¹³ Nonetheless, the atmospheric budget for HAc is poorly constrained, and atmospheric models consistently fail to replicate observed distributions in the atmosphere.^{7,14}

In the UT/LS, the only significant loss process for HAc is thought to be reaction with OH radicals. The reaction of $\text{OH} + \text{CH}_3\text{COOH}$ proceeds mainly via abstraction of the acidic hydrogen (eq 1a)¹⁵



Received: January 5, 2011

Revised: March 1, 2011

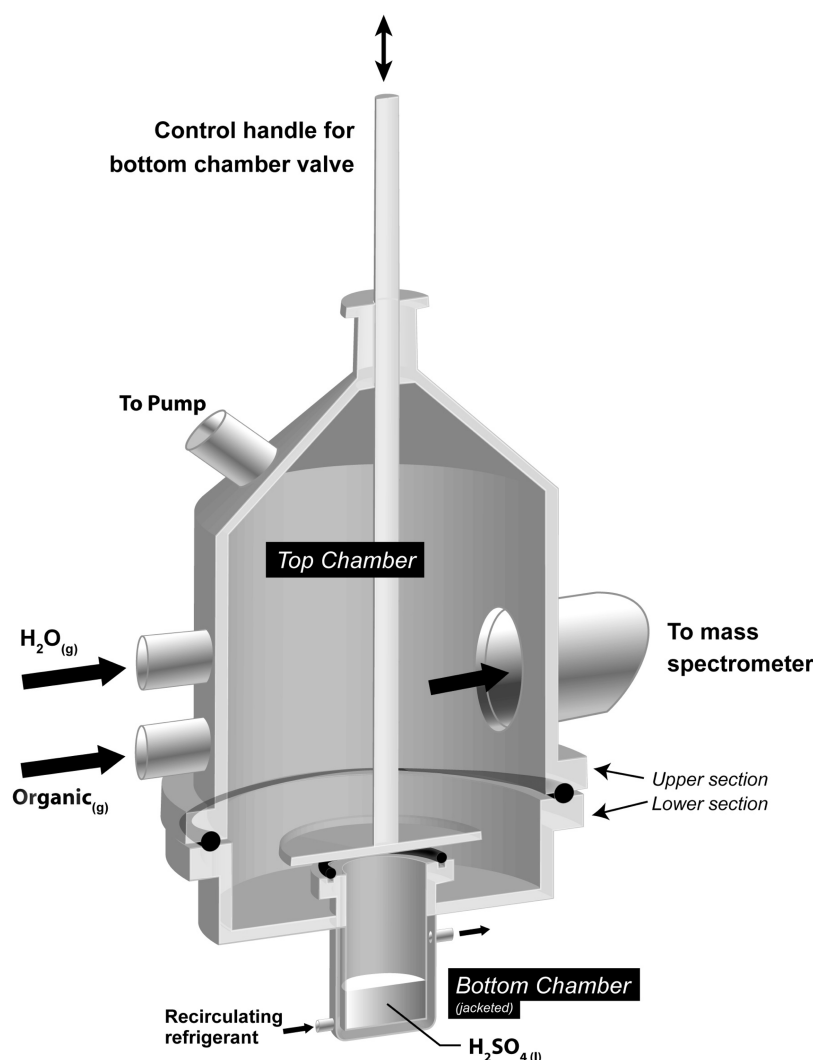


Figure 1. Cross-sectional diagram of the Pyrex Knudsen cell used in this work. The upper and lower sections are sealed using a large McCarter clamp (not shown). The bottom chamber is jacketed with a recirculating coolant. Exposure of the organic vapor to the sulfuric acid surface is initiated by raising the central piston, which opens a lid to the lower chamber.

In air, the methyl radicals generated in reaction channel 1a are rapidly converted to methylperoxy radicals by reaction with O_2 . It has been suggested that HAC, with an estimated UT lifetime with respect to reaction with OH radicals of 9.4 days, could be as significant a source of methyl peroxy radicals as methane in influencing HO_x budget of the UT.¹⁵ In the UT/LS, the HO_x radicals participate in the production of ozone and oxidation of SO_2 to H_2SO_4 , which can generate new aerosols. This raises the question as to the importance of uptake on acidic UT/LS aerosols as a loss process for HAC.

Acetic acid's halogenated analogue, CF_3COOH (trifluoroacetic acid, TFA), is produced as an atmospheric degradation product from the oxidation of hydrochlorofluorocarbons (HCFCs), hydrofluorocarbons (HFCs), and long chain polyfluorinated compounds (PFCs).^{16,17} TFA is produced through hydrolysis of acetyl fluorides/chlorides in aqueous phase rain–cloudwater chemistry, highly soluble in water,¹⁸ and expected to be removed from the atmosphere mainly by washout. Upon evaporation of cloudwater, TFA will be released into the gas phase and subsequent removal will occur by reincorporation into cloudwater or by aerosol/surface/ocean deposition. Like HAC, TFA

does not undergo photolysis, but reaction with OH radicals provides only a minor sink for TFA.¹⁹

To improve our understanding of the fate of HAC and TFA in the UT/LS we conducted an experimental study of the solubility of HAC and TFA in low-temperature aqueous sulfuric acid solutions representative of typical UT/LS particulates. Results are discussed with respect to the composition of UT/LS aerosols and the atmospheric processing of HAC and TFA.

2. EXPERIMENTAL METHODS

The apparatus and experimental techniques used in this work have been described previously in detail.²⁰ Uptake of the organic acids was measured using a classic Knudsen cell apparatus consisting of two Teflon-coated Pyrex chambers separated by an internal valve, as shown in Figure 1. The pressure in the Knudsen cell was monitored using a capacitance manometer pressure gauge. The bottom, jacketed chamber was cooled with circulating ethanol and filled with several milliliters of an aqueous H_2SO_4 solution of desired concentration. A magnetic stir bar in

the H₂SO₄ solution allowed for mixing of the sample (≥ 15 min) between successive experiments. At the beginning of each experiment, a linear relationship was determined between the mass spectrometer signal at $m/z = 18$ and the vapor pressure of water. The pressure was measured by the capacitance manometer in the absence of any organic acids. The calibrated $m/z = 18$ signal was then employed during each experiment to determine the water vapor pressure in the presence of the organic gas of interest. The temperature of the sulfuric acid solution was measured using two thermocouples mounted on the outside of the bottom chamber walls. The thermocouples were calibrated daily by comparing the vapor pressure of water above the H₂SO₄ solution (before introduction of the organic acid) with the vapor pressure predicted by the Aerosol Inorganics Model.^{21–23} Applied corrections were in the range of 1–3 K. The uncertainty in the temperature measurements is estimated to be no larger than ± 1 K, mostly due to an uncertainty of approximately 0.1 mTorr in the water vapor pressure measurements. Since the lower chamber of the Knudsen cell is cold, but the walls of the upper chamber are approximately at room temperature, thermal transpiration may be a source of systematic error in our temperature data (water vapor pressure). However, the magnitude of this effect in our system was discussed by Michelsen et al.²⁴ and found to be insignificant when compared to the uncertainties in the diffusion coefficients and determination of the slope of the γ^{-1} data (see below for definitions).

Sulfuric acid solutions were prepared by dilution of commercial 96 wt % H₂SO₄ stock solution (Merck) and deionized water, and final solution concentrations of 75.0 ± 0.2 , 74.4 ± 0.1 , 58.0 ± 0.1 , 57.8 ± 0.1 , 40.7 ± 0.1 , and 40.1 ± 0.1 wt % H₂SO₄ were determined by titration with 5.00 M sodium hydroxide standard (VWR). All other reagents were obtained from commercial sources at purities $>99\%$. Gas-phase HAC and TFA (Aldrich) and reagent grade water (Aldrich) were taken from the vapor above liquid samples which were stored with molecular sieves and purified with at least one freeze–pump–thaw cycle before each experiment.

The top chamber of the Knudsen cell is interfaced with a differentially pumped mass spectrometer (Balzers QMG 421C electron ionization quadrupole system) through a calibrated aperture. Gaseous water and organic acid were admitted to the top chamber of the cell through separate capillaries and exited via the aperture. To prevent changes in the H₂SO₄ solution composition, water vapor in the cell was matched to the vapor pressure of the sulfuric acid solutions. Total pressure in the cell was usually ≤ 25 mTorr to ensure that the mean free path of the gas molecules was longer than or comparable to the diameter of the escape aperture (0.250 cm).

Separate experiments were conducted using either HAC or TFA. Once stable flows in the upper chamber were established for water and the organic acid, exposure to the sulfuric acid surface was initiated by opening the valve separating the two chambers. Uptake of the organic acid was then observed as a decrease in the mass spectrometer signal. Mass fragments observed were $m/z = 60$ (CH₃COOH⁺), 45 (COOH⁺), and 43 (CH₃CO⁺) for HAC and $m/z = 69$ (CF₃⁺), 50 (CF₂⁺), and 45 (COOH⁺) for TFA. For maximum experimental sensitivity, we chose to monitor the molecular peak at $m/z = 60$ and the characteristic base peak at $m/z = 45$ (COOH⁺) for HAC and TFA, respectively.

The net uptake coefficient, γ , is defined as the fraction of incident molecules taken up by the surface and is calculated from the raw data²⁰

$$\gamma = \frac{A_h}{A_s} \left(\frac{F_o - F}{F} \right) \quad (2)$$

The number of molecules lost to the surface is measured by the change in flow to the mass spectrometer upon exposure, $F_o - F$, where F_o is the flow prior to exposure and F is the flow during exposure. The mass spectrometer signal is proportional to the flow of molecules out of the cell. Hence, this signal can be used directly for calculation of γ . A_h is the area of the escape aperture (0.049 cm²), and A_s is the surface area of the sulfuric acid in the bottom chamber (5.55 cm²). The rate of organic acid diffusion into the bulk liquid combined with the overall solubility and any reaction which occurs controls the time dependence of γ ²⁵

$$\frac{1}{\gamma} = \frac{1}{\Gamma_g} + \frac{1}{\alpha} + \frac{\sqrt{\pi}\bar{c}}{4RTH^*\sqrt{D}} \left(\frac{1}{t^{-1/2} + \sqrt{\pi k}} \right) \quad (3)$$

where t is time, \bar{c} is the average molecular velocity, R is the universal gas constant, T is the absolute temperature, D is the liquid-phase diffusion coefficient of HAC or TFA, α is the mass accommodation coefficient, k is the pseudo-first-order rate constant for any irreversible reaction (loss), and Γ_g characterizes any limitation due to gas-phase diffusion. Note that the *effective* Henry's law solubility coefficient, H^* , is used since solution-phase HAC and TFA may undergo further reversible reactions in solution. The quantity $H^*(D)^{1/2}$ can be determined from the reciprocal of the slope of a plot of γ^{-1} versus $(t)^{1/2}$, and H^* can then be determined if the diffusion coefficient is known. Diffusion coefficients employed in this work were calculated according to $D = cT/\eta$, where the constant c was calculated to be 4.9 and 4.3×10^{-8} mol cm K⁻¹ s⁻² using a Le Bas molecular volume²⁶ of 64.1 and 79.7 cm³ mol⁻¹ for HAC and TFA, respectively. H₂SO₄ viscosities, $\eta(T)$, were calculated from the parametrization of Williams and Long.²⁷ For all experiments, data at $(t)^{1/2} < 7$ s^{1/2} were excluded in the data analysis because eq 3, which is a linear approximation to coupled differential equations that describe the uptake processes soon after the valve is opened, does not apply at short times.^{27,28} Values of H^* along with experimental conditions, calculated values of D , and the derived thermodynamic parameters are reported in Tables 1 and 2 and discussed in the following sections.

3. RESULTS AND DISCUSSION

Typical data obtained from experiments investigating the uptake of HAC and TFA in H₂SO₄ are shown in Figures 2 and 3. Figure 2A shows the mass spectrometer signal ($m/z = 60$) as a function of time as gas-phase HAC was exposed to 57.8 wt % H₂SO₄ at 238.2 K. Exposure began at $t = 0$ s and ended after approximately 330 s. As seen in Figure 2A, the signal recovers slightly but does not approach its initial intensity during the duration of these experiments. Figure 2B shows the inverse of the calculated uptake coefficient, γ , plotted versus the square root of time. Using eq 3 with $k = 0$, the Henry's law coefficient can be determined from the slope ($= H^*D^{1/2}$) of the linear regression to the data. The data points used for the regression are indicated with solid circles. For the experiment shown here, we obtain $H^* = 9.6 \times 10^5$ M atm⁻¹.

Table 1. Measured H^* for the Uptake of Acetic Acid (HAc) and Trifluoroacetic Acid (TFA) into Aqueous Sulfuric Acid Solutions

| H ₂ SO ₄ /H ₂ O composition | solute | T (K) | D (cm ² s ⁻¹) | H* (M atm ⁻¹) |
|--|--------|-------|--------------------------------------|---------------------------|
| 74.4 wt % | HAc | 219.6 | 5.04×10^{-9} | 3.8×10^8 |
| | | 231.2 | 2.43×10^{-8} | 3.6×10^7 |
| | | 231.2 | 2.43×10^{-8} | 3.5×10^7 |
| | | 231.2 | 2.43×10^{-8} | 3.0×10^7 |
| | | 237.4 | 4.58×10^{-8} | 1.3×10^7 |
| | | 237.4 | 4.58×10^{-8} | 1.3×10^7 |
| | | 237.4 | 4.58×10^{-8} | 1.3×10^7 |
| | | 244.3 | 8.32×10^{-8} | 5.0×10^6 |
| | | 244.3 | 8.32×10^{-8} | 4.6×10^6 |
| | | 244.3 | 8.32×10^{-8} | 4.8×10^6 |
| 75.0 wt % | TFA | 225.5 | 9.36×10^{-9} | 3.3×10^4 |
| | | 226.6 | 1.08×10^{-8} | 2.4×10^4 |
| | | 226.6 | 1.08×10^{-8} | 1.5×10^4 |
| | | 227.3 | 3.61×10^{-8} | 5.9×10^3 |
| | | 240.4 | 4.80×10^{-8} | 6.1×10^3 |
| | | 242.5 | 5.79×10^{-8} | 1.7×10^3 |
| 57.8 wt % | HAc | 218.1 | 6.24×10^{-8} | 5.2×10^7 |
| | | 218.1 | 6.24×10^{-8} | 3.7×10^7 |
| | | 218.1 | 6.24×10^{-8} | 4.4×10^7 |
| | | 225.7 | 1.18×10^{-7} | 9.1×10^6 |
| | | 225.7 | 1.18×10^{-7} | 1.0×10^7 |
| | | 225.7 | 1.18×10^{-7} | 1.2×10^7 |
| | | 229.1 | 1.57×10^{-7} | 6.0×10^6 |
| | | 229.1 | 1.57×10^{-7} | 6.3×10^6 |
| | | 229.1 | 1.57×10^{-7} | 5.3×10^6 |
| | | 232.1 | 1.94×10^{-7} | 1.7×10^6 |
| | | 232.1 | 1.94×10^{-7} | 2.3×10^6 |
| | | 232.1 | 1.94×10^{-7} | 1.7×10^6 |
| | | 238.2 | 2.86×10^{-7} | 9.0×10^5 |
| | | 238.2 | 2.86×10^{-7} | 9.6×10^5 |
| | | 238.2 | 2.86×10^{-7} | 8.7×10^5 |
| | | 245.0 | 4.24×10^{-7} | 3.2×10^5 |
| | | 245.0 | 4.24×10^{-7} | 2.4×10^5 |
| | | 245.0 | 4.24×10^{-7} | 2.2×10^5 |
| 58.0 wt % | TFA | 218.0 | 5.32×10^{-8} | 2.0×10^6 |
| | | 218.0 | 5.32×10^{-8} | 1.8×10^6 |
| | | 220.5 | 6.70×10^{-8} | 1.0×10^6 |
| | | 225.9 | 1.06×10^{-7} | 2.4×10^5 |
| | | 226.0 | 1.06×10^{-7} | 2.9×10^5 |
| | | 226.1 | 1.07×10^{-7} | 2.4×10^5 |
| | | 232.3 | 1.69×10^{-7} | 9.9×10^4 |
| | | 232.3 | 1.69×10^{-7} | 9.4×10^4 |
| | | 232.3 | 1.69×10^{-7} | 1.0×10^5 |
| | | 239.6 | 2.70×10^{-7} | 1.9×10^4 |
| | | 207.4 | 5.25×10^{-8} | 1.4×10^8 |
| 40.1 wt % | HAc | 207.4 | 5.25×10^{-8} | 7.3×10^7 |
| | | 215.0 | 1.02×10^{-7} | 1.3×10^7 |
| | | 221.7 | 2.10×10^{-7} | 3.2×10^6 |
| | | 221.7 | 2.10×10^{-7} | 2.9×10^6 |
| | | 221.7 | 2.10×10^{-7} | 4.2×10^6 |

Table 1. Continued

| H ₂ SO ₄ /H ₂ O composition | solute | T (K) | D (cm ² s ⁻¹) | H* (M atm ⁻¹) |
|--|--------|-------|--------------------------------------|---------------------------|
| 40.7 wt % | TFA | 207.8 | 4.75×10^{-8} | 3.6×10^8 |
| | | 214.5 | 9.52×10^{-8} | 4.5×10^7 |
| | | 221.2 | 1.74×10^{-7} | 7.1×10^6 |
| | | 221.2 | 1.74×10^{-7} | 5.2×10^6 |
| | | 226.7 | 2.59×10^{-7} | 1.8×10^6 |
| | | 226.7 | 2.59×10^{-7} | 3.0×10^6 |
| | | 226.7 | 2.59×10^{-7} | 1.8×10^6 |
| | | 226.7 | 2.59×10^{-7} | 3.0×10^6 |

Figure 3 shows the results from an analogous experiment employing TFA exposed to 58.0 wt % H₂SO₄ at 232.3 K (Figure 3A) and with the inverse of the uptake coefficient plotted as a function of the square root of exposure time (Figure 3B). For the experiment shown here, we obtain $H^* = 9.4 \times 10^4$ M atm⁻¹.

The effective Henry's law coefficients determined from the time-dependent uptake experiments are plotted in Figure 4 as $\log(H^*)$ versus inverse temperature. A summary of the data obtained in this work is given in Table 1. For the conditions studied in this work (40.1–75.0 wt % H₂SO₄, 207.4–245.0 K), the solubility of HAc and TFA varies from 10⁵ to 10⁸ M atm⁻¹ and from 10³ to 10⁸ M atm⁻¹, respectively. As seen from Figure 4, the amount of HAc/TFA dissolution varies greatly with acidity. With increasing H₂SO₄ concentration, the solubility of acetic acid increases while that for the fluorinated analog decreases. Significant dissociation of the organic acids is not expected to occur in these highly concentrated H₂SO₄ solutions.

For comparison, the extrapolated (hypothetical) solubilities of HAc and TFA in water are also shown in Figure 4 as dashed cyan lines (molecular solubility only), based on extrapolation from the solubility in water at 275–308 K, down to the temperatures employed in this work.^{18,29} The dash-dotted cyan line in Figure 4B includes the dissociation of TFA ($pK_a = 0.23$; 298 K³⁰), which increases the estimated overall solubility, i.e., H^* for TFA, by a factor of 10⁶ relative to that of molecular solubility alone for a given partial pressure in the gas phase. The average overall uncertainty in our values for H^* is estimated to be $\pm 20\%$. The main sources of error are the uncertainty in the diffusion coefficient (10–20%),³¹ which is highest for the most viscous solutions, and the error in determining the slope of the $1/\gamma$ data ($\pm 10\%$).

At UT/LS temperatures, TFA is substantially less soluble in H₂SO₄ than in water, similar to behavior that has been found for strong inorganic acids, e.g., HCl and HBr.^{32,33} However, the picture is rather different for HAc. For the 57.8 and 40.1 wt % H₂SO₄ solutions, the solubility of HAc is barely less than that in water (dashed line) at the warmer end of the experimental conditions and more soluble at the colder end. Furthermore, the 74.1 wt % data show increased solubility significantly above the extrapolated (hypothetical) solubility in water (dashed line). The increased solubility of oxygenated organics at higher acidity has often been attributed to protonation of one or more oxygen atoms, allowing more of the gas to be taken up into solution.^{34–36} Carboxylic acids can undergo protonation reactions, with the resulting positive charge being delocalized over both oxygens.³⁷ It is likely that the carbonyl oxygen in HAc undergoes some degree of protonation in the concentrated H₂SO₄.³⁸ In contrast, the presence of electron-withdrawing fluorine substituents near the site of protonation likely prohibit or substantially limit this

Table 2. Thermodynamic Parameters for HAc and TFA Acid Dissolution in Aqueous Sulfuric Acid (parameters given in parentheses are calculated based on results stated in the cited literature)

| solute | H ₂ SO ₄ (wt %) | $\alpha_{\text{H}_2\text{SO}_4}$ | M_{soln}^a (mol L ⁻¹) | Figure 4 fits (un-/constrained) | | | ΔH° (un-/constrained) (kJ mol ⁻¹) | ΔS° (un-/constrained) (J mol ⁻¹ K ⁻¹) |
|--------|---------------------------------------|----------------------------------|--|---------------------------------|-----------------|-----------|---|--|
| | | | | a (slope) | b (intercept) | R^2 | | |
| HAc | 0 | 0.00 | 55.6 | | | | (-52) ^b | (-129) ^c |
| | 40.1 | 0.11 | 45.31 | 4.74/2.63 | -14.9/-5.08 | 0.96/0.78 | -90.8/-50.4 | -317.0/-129 |
| | 57.8 | 0.20 | 36.12 | 4.48/2.70 | -12.9/-5.18 | 0.99/0.83 | -85.8/-51.8 | -276.8/-129 |
| | 74.4 | 0.35 | 24.71 | 4.02/2.97 | -9.81/-5.34 | 0.99/0.92 | -77.0/-56.8 | -214.6/-129 |
| TFA | 0 | 0.00 | 55.6 | | | | -77.6 ^d | (-184.6) ^e |
| | 40.7 | 0.11 | 45.04 | 5.32/3.30 | -17.2/-8.74 | 0.88/0.81 | -101.8/-63.2 | -361.2/-184.6 |
| | 58.0 | 0.20 | 36.00 | 4.64/3.06 | -15.0/-8.84 | 0.99/0.87 | -88.8/-58.6 | -317.7/-184.6 |
| | 75.0 | 0.36 | 24.23 | 3.12/2.85 | -9.42/-9.01 | 0.95/0.87 | -59.8/-54.6 | -206.9/-184.6 |

^a Calculated at 220 K. ^b From Johnson et al.²⁹ ^c From Wilson et al.⁴⁶ ^d From Bowden et al.¹⁸ ^e Calculated based on ΔH° in Bowden et al.¹⁸

reaction from occurring,³⁹ resulting in the decrease in solubility of TFA with increasing acidity.

We can estimate the degree of protonation for HAc in our experiments using eq 4, where $[\text{HAcH}^+]$ is the concentration of the protonated HAc and pK_{HAcH^+} is the protonation constant. The quantity X is the excess acidity for sulfuric acid,⁴⁰ and m^* is the excess acidity slope (2.14 for propanoic acid).⁴¹

$$\log \frac{[\text{HAcH}^+]}{[\text{HAc}]} = \log[\text{H}^+] + m^*X + pK_{\text{HAcH}^+} \quad (4)$$

The only value available in the literature for HAc basicity is a half-protonation value of -6.75 based on the Hammett acidity scale.⁴² Using the slope of the corresponding Hammett plot for HAcH^+ , the half-protonation value can be converted into a value of pK_{HAcH^+} and adjusted for the temperature dependence based on the protonation enthalpy for HAc. Unfortunately, neither the Hammett plot nor the protonation enthalpy for HAc is known. Assuming a slope similar to that of propanoic acid (0.37),⁴¹ we estimate a pK_{HAcH^+} of approximately -2.5. In the absence of a known protonation enthalpy for HAc, we use that of methyl acetate (-18.8 kJ mol⁻¹) as a reasonable approximation,⁴³ arriving at $pK_{\text{HAcH}^+} \approx -3.7$ at 220 K for HAc. Thus, on the basis of eq 4, we predict that HAc is 98% protonated in 40 wt % sulfuric acid at 200 K. Even though there is substantial uncertainty in this prediction, it indicates that protonation of HAc is nearly complete even in our most dilute H₂SO₄ solution. Therefore, it is unlikely that protonation is the main explanation for the increasing solubility for HAc with increasing acidity. Instead, the simplest explanation for the increasing solubility for HAc with increasing acidity would be that H₂SO₄ is more efficient at solvating oxygenated organic compounds than is water.⁴⁴

Figure 4 also provides information on the thermodynamics of HAc and TFA dissolution in cold, aqueous H₂SO₄. The enthalpy of solvation (ΔH°) can be determined using eqs 5–7³⁶

$$\log(H^*) = a \times \frac{1000}{T} + b \quad (5)$$

$$a = \frac{\Delta H^\circ}{2.303R} \quad (6)$$

$$b = \frac{\Delta S^\circ}{2.303R} + \log(M_{\text{soln}}) \quad (7)$$

where a and b are the slope and intercept, respectively, of the linear fits, ΔS° is the entropy of solvation, R is the gas constant, and M_{soln} is the molarity of water in the solutions, calculated at 220 K.⁴⁵ As shown in Table 2 (ΔH° , unconstrained values), both solutes show a *positive* correlation for ΔH° with increasing H₂SO₄ concentration. We find that $\Delta H^\circ(\text{HAc}) = -90.8$, -85.8 , and -77.0 kJ mol⁻¹ for 40.1, 57.8, and 74.4 wt % H₂SO₄, while $\Delta H^\circ(\text{TFA}) = -101.8$, -88.8 , and -59.8 kJ mol⁻¹ for 40.7, 58.0, and 75.0 wt % H₂SO₄. The fits to our data are very good ($R^2 = 0.96$, 0.99 , and 0.99 for HAc, 0.88 , 0.99 , and 0.95 for TFA), but a significant difference exists between the calculated entropy values (Table 2) and the literature values for uptake into water (-129 and -184.6 J mol⁻¹ K⁻¹ for HAc and TFA, respectively). Although protonation occurs for HAc, and additional ordering of the solvent at higher acidities should result in more negative entropy values for both solutes, the magnitude of the deviations in dissolution entropy observed here relative to dissolution in water is quite unexpected. The largest differences in ΔS° (relative to water) appear for our most dilute H₂SO₄ solutions, something that has also been observed for uptake of other organics into strong H₂SO₄ solutions.^{24,44} The large negative entropies observed suggest that the organic acids are losing significantly more entropy than would be expected from even simple solvation in water followed by ionization (e.g., -221 J mol⁻¹ K⁻¹ for HAc⁴⁶), and may be interpreted as a considerable ordering of the solvent around the solute (allowing carboxylic acids to establish hydrogen-bonded interactions). Gas phase dimerization of carboxylic acids is well-known,^{47,48} but at low acid concentrations in water no dimer structure exists.⁴⁹ It is conceivable that some kind of carboxylic acid-H₂SO₄ dimer complex could form in concentrated H₂SO₄ solutions thereby substantially lowering ΔS° .

It would be fair to point to the fact that the temperature range employed here may not be large enough to determine ΔS° with an acceptable degree of certainty, since our data are located far away from the ordinate axis. Thus, it is not clear whether our observed values of ΔS° are real or simply an experimental artifact due to the limited temperature range, again most pronounced for the more dilute H₂SO₄ solutions. To counter this limitation, it has become customary^{24,34,44} simply to constrain the fits by fixing the value of ΔS° to that for dissolution in water.

On the basis of our discussion above, we chose to perform both a constrained and unconstrained linear least-squares fit to the data, in the former case fixing the y -axis intercept according to the values of ΔS° for dissolution in water, and report

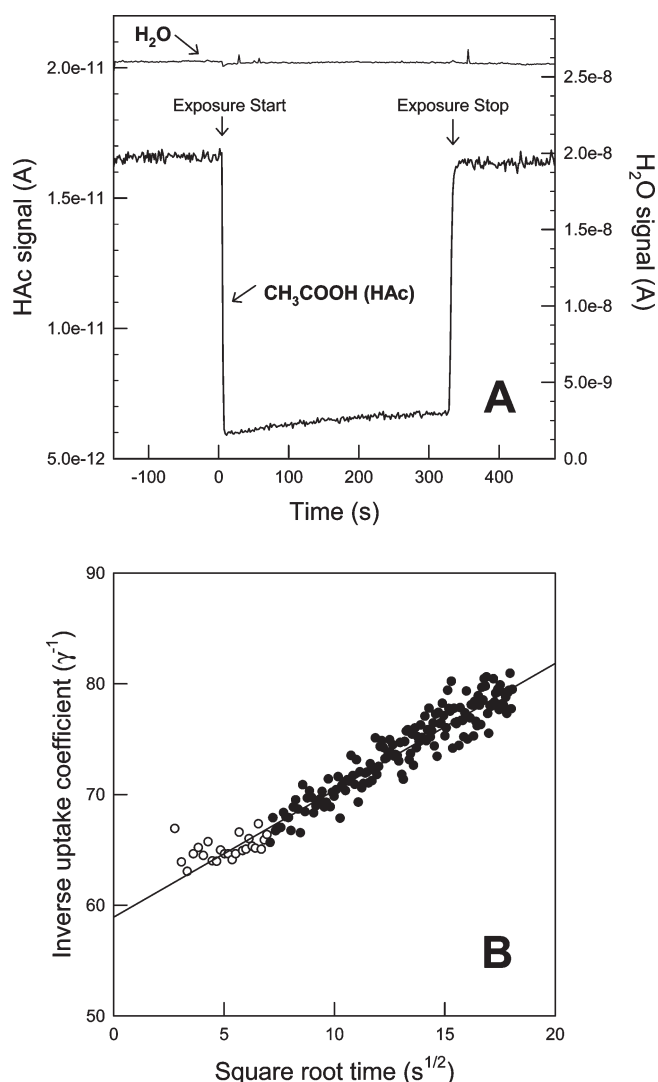


Figure 2. (A) Mass spectrometer signal ($m/z = 60$) for HAc before, during, and after exposure to 57.8 wt % H_2SO_4 at 238.2 K. Exposure was initiated at $t = 0$ s. (B) Inverse of the uptake coefficient, γ , for the experiment shown in A, plotted as a function of the square root of exposure time. The data points used for the regression are indicated with solid circles.

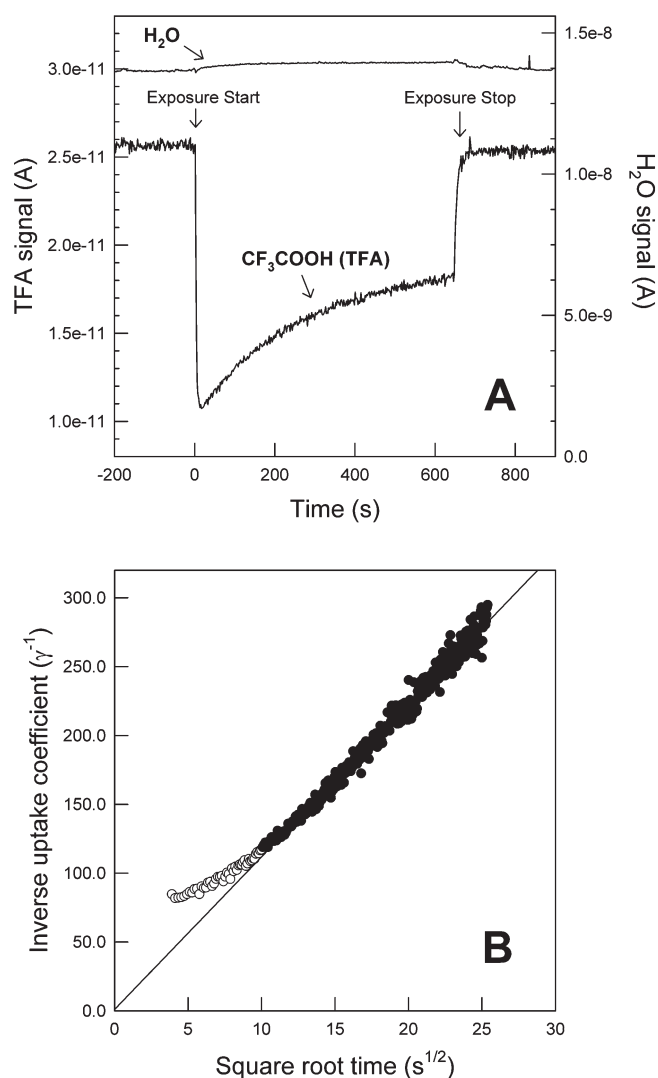


Figure 3. (A) Mass spectrometer signal ($m/z = 45$) for TFA before, during, and after exposure to 58.0 wt % H_2SO_4 at 232.3 K. Exposure was initiated at $t = 0$ s. (B) Inverse of the uptake coefficient, γ , for the experiment shown in A, plotted as a function of the square root of exposure time. The data points used for the regression are indicated with solid circles.

thermodynamic parameters for both the constrained and unconstrained linear least-squares fits (see Table 2). Using -129 and $-184.6 \text{ J mol}^{-1} \text{ K}^{-1}$ for $\Delta S^\circ(\text{HAc})$ and $\Delta S^\circ(\text{TFA})$, respectively,^{18,46} we obtain values of enthalpy of $\Delta H^\circ(\text{HAc}) = -50.4, -51.8,$ and $-56.8 \text{ kJ mol}^{-1}$ for 40.1, 57.8, and 74.4 wt % H_2SO_4 , while $\Delta H^\circ(\text{TFA}) = -63.2, -58.6,$ and $-54.6 \text{ kJ mol}^{-1}$ for 40.7, 58.0, and 75.0 wt % H_2SO_4 . As shown in Figure 4, the constrained linear least-squares fits produce reasonably strong correlations ($R^2 = 0.78, 0.83,$ and 0.92 for HAc and $0.81, 0.87,$ and 0.87 for TFA). Using the constrained fitting method, the resulting values for $\Delta H^\circ(\text{TFA})$ continue to show a positive correlation with increasing H_2SO_4 concentration, as they did with the unconstrained fitting method. However, acetic acid shows the opposite trend in $\Delta H^\circ(\text{HAc})$, with a negative correlation between $\Delta H^\circ(\text{HAc})$ and increasing sulfuric acid concentration. Although the reason for this difference between HAc and TFA, when using the constrained fitting method, is not entirely clear, the increasingly negative values of $\Delta H^\circ(\text{HAc})$ in more

concentrated sulfuric acid solutions can be explained by sulfuric acid being a better solvent than water for HAc. The degree of the change in $\Delta H^\circ(\text{HAc})$, obtained here using the constrained fitting method, is similar to that reported for several other organics^{34,36} and contrasts the behavior of inorganic strong acids, e.g., HBr, HCl, and HNO_3 .^{27,32,50}

By fixing $T = 220 \text{ K}$, a temperature in the middle of the experimental range, empirical fits to the effective Henry's law coefficients yield parametrized expressions, eqs 8a and 8b, where $x_{\text{H}_2\text{SO}_4}$ is the mole fraction of H_2SO_4 in the solution that can be used to determine the solubility of HAc or TFA in H_2SO_4 at conditions other than those studied here

$$H^*(\text{HAc}) = 2.501 \times 10^6 + 1.110 \times 10^6 \times \exp(15.89 \times (x_{\text{H}_2\text{SO}_4})) \quad (8a)$$

$$H^*(\text{TFA}) = 4.378 \times 10^5 + 5.997 \times 10^{-8} \times \exp(-38.54 \times (x_{\text{H}_2\text{SO}_4})) \quad (8b)$$

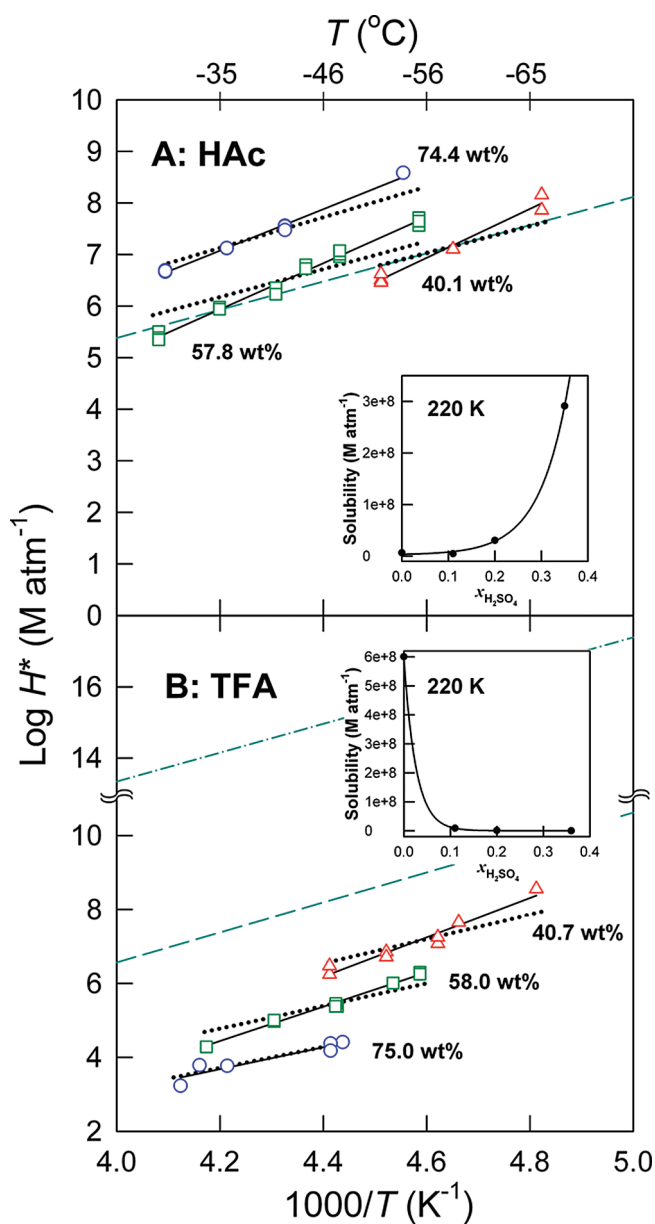


Figure 4. Effective Henry's law coefficient for HAc (A) and TFA (B) as a function of inverse temperature and acid composition (H_2SO_4 weight percentages). Solid black lines are linear least-squares fit to the data, while dotted lines are fits with fixed $\Delta S = -129$ (A) and -184.6 (B) $\text{J mol}^{-1} \text{K}^{-1}$. Dashed cyan lines indicate the solvation (physical solubility only) of HAc and TFA in water, while the dash-dotted cyan line includes both solvation and dissociation of TFA in water (see text for details). The inserts show solubility of HAc and TFA as a function of H_2SO_4 mole fraction, $x_{\text{H}_2\text{SO}_4}$ ($T = 220 \text{ K}$).

When utilizing eqs 8a and 8b care should be taken not to extrapolate beyond the acid compositions used in this study ($0.11 < x_{\text{H}_2\text{SO}_4} < 0.36$), as these equations may not apply outside the range of acidities studied. The parametrized solubilities are plotted versus acid composition in the inserts in Figure 4.

4. ATMOSPHERIC IMPLICATIONS

The large solubility of acetic acid in cold aqueous sulfuric acid means that even though it is a minor trace gas in the UT/LS, it

may be an important trace constituent in UT/LS particles. Detailed information on gas- and particulate-phase HAc mixing ratios in the boundary layer and the free troposphere exists in the literature; however, for higher altitudes the literature is sparse in measurements. During the 1991/1994 Pacific Exploratory Mission West phases A and B (PEM-West A and B), median mixing ratios between 73 and 630 pptv in the altitude range of 7–12 km were measured over the Pacific Ocean,⁵¹ and in a 1991 aircraft campaign in the UT/LS over Germany, Reiner et al.⁵² measured mean mixing ratios between 110 and 357 pptv at altitudes of 7–11.3 km. The altitude profile showed a maximum at 9 km with the tropopause determined to be located between 9.3 and 11.5 km altitude (from the atmospheric temperature profile). Subsequently, during the 1992 TRansport and Atmospheric Chemistry near the Equatorial Atlantic (TRACE-A) mission over the tropical South Atlantic,⁵³ HAc concentrations as high as 8 ppbv were measured, with average values of 2–3 ppbv throughout the 0–12 km column (8–12 km median of 1900 pptv).

There are no measurements of TFA mixing ratios in the upper troposphere or lower stratosphere.

Using the solubilities determined in this work, we can determine the expected impact of sulfate aerosols on UT/LS concentrations of HAc and TFA. Assuming characteristic mid-latitude UT sulfate particles (220 K, 65 wt %), the value determined here for acetic acid, $H^* = 7 \times 10^7 \text{ M atm}^{-1}$, suggests that uptake by sulfate would account for $\sim 1 \times 10^{-3} \%$ of total UT HAc under volcanically quiescent conditions but for more than 1% of total UT HAc under high sulfate perturbations (Mt. Pinatubo-like conditions). In comparison, the fractions of total atmospheric TFA that would reside in sulfate aerosols under those two types of conditions are $\sim 1 \times 10^{-5} \%$ and $\sim 1 \times 10^{-2} \%$, respectively.

The equilibrium organic content for a typical UT sulfate particle (0.1 μm radius, 220 K, 58 wt % H_2SO_4 , 12 km, 160 Torr or 213 hPa) has been calculated from the background mixing ratios of a set of oxygenated organic compounds (800 pptv methanol, 70 pptv ethanol, 600 pptv acetone, 50 pptv formaldehyde, 80 pptv acetaldehyde) and their measured solubilities.²⁴ Adopting this same approach and assuming an estimated mixing ratio of 300 pptv,⁵² we calculate an equilibrium liquid-phase concentration of $3.6 \times 10^{-4} \text{ M}$ HAc. Because of the large H^* for HAc, the concentration of HAc is also very large. In fact, the HAc concentration is up to 4 orders of magnitude greater than those calculated for any of the other compounds in the set. On the basis of this, HAc is responsible for more than 3/4 of the particle organic content by mass, as calculated for the six organics listed above. For a typical LS particle radius of 0.1 μm , this corresponds to approximately 1000 HAc molecules per particle. Still, the total organic mass fraction due to dissolution of these six gases listed above is less than 0.002% of the particle mass; therefore, simple solubility of OVOCs cannot account for the organic matter detected in UT/LS particles by Murphy et al.² Other compounds, mechanisms, and/or reaction pathways may also be responsible for the accumulation of organic matter in UT/LS particles.

5. CONCLUSIONS

These are the first measurements of acetic acid and trifluoroacetic acid solubilities in sulfuric acid solutions under UT/LS conditions. The solubilities were measured over ranges of temperature (207–245 K) and acid composition (40.1–75.0 wt % H_2SO_4). For both acetic acid (HAc) and trifluoroacetic acid

(TFA), H^* is inversely dependent on temperature. Solubility increases for HAc with increasing acidity but decreases for TFA. Measured values of H^* range from $1.7 \times 10^3 \text{ M atm}^{-1}$ for TFA in 75.0 wt % H_2SO_4 at 242.5 K to $3.8 \times 10^8 \text{ M atm}^{-1}$ for HAc in 74.4 wt % H_2SO_4 at 219.6 K. On the basis of literature data, we find that acetic acid acts as a base in the sulfuric acid solutions studied here, with essentially all HAc in the protonated form (HAcH^+) when sulfuric acid is $\geq 40 \text{ wt } \%$. In comparison, protonation of TFA to CF_3COOH^+ is likely minimal. The increased solubility of HAc with increasing H_2SO_4 concentration cannot be explained by increased protonation in the stronger H_2SO_4 solutions. It is possible that H_2SO_4 simply is a better solvent than water for oxygenated organic compounds.

The enthalpy of solvation (ΔH°) of HAc and TFA dissolution in cold, aqueous H_2SO_4 was determined using two different fitting schemes. Unconstrained fits produced significant differences between the calculated entropy values and the literature values for uptake into water. Constrained fits, using the values of ΔS° for dissolution in water, resulted in values of ΔH° for HAc and TFA, which differed in trends with increasing sulfuric acid concentrations. In effect, in strong sulfuric acid solutions, HAc behaves similarly to an oxygenated organic compound, e.g., ethanol, and TFA behaves similarly to a strong inorganic acid, e.g., HCl. Computational studies may help in elucidating the factors responsible for determining the thermodynamics of dissolution of organic acids into cold, aqueous H_2SO_4 .

The high solubility of HAc means that it will appear as a trace constituent in UT/LS particles. For a typical UT sulfate particle, we calculate an equilibrium liquid-phase concentration of $3.6 \times 10^{-4} \text{ M}$ HAc. Gas-phase TFA will only very sparingly partition into UT/LS particles.

AUTHOR INFORMATION

Corresponding Author

*M.P.S.A.: E-mail, mads@sulbaek.dk. L.T.I.: E-mail, laura.tiraci@nasa.gov.

Present Addresses

^{||}Now at Jet Propulsion Laboratory, California Institute of Technology, California.

[⊥]Now at Department of Chemistry and Biochemistry, University of Colorado, Boulder.

ACKNOWLEDGMENT

This work was funded by the NASA Upper Atmosphere Research and New Investigator Programs. M.P.S.A. and O.J.N. would like to thank the Danish Research Agency for a research grant and the Villum Kann Rasmussen Fund for financial support. R.R.H.M. was a National Research Council Associate, and J.L.A. was supported by the NASA Undergraduate Student Research Program. The authors thank D. R. Blake and F. S. Rowland (UC Irvine) for helpful comments.

REFERENCES

- (1) Solomon, S. *Rev. Geophys.* **1988**, *26*, 131.
- (2) Murphy, D. M.; Thompson, D. S.; Mahoney, M. J. *Science* **1998**, *282*, 1664.
- (3) DeMott, P. J.; Cziczko, D. J.; Prenni, A. J.; Murphy, D. M.; Kreidenweis, S. M.; Thomson, D. S.; Borys, R.; Rogers, D. C. *Proc. Natl. Acad. Sci. U.S.A.* **2003**, *100*, 14655.
- (4) Noziere, B.; Esteve, W. *Geophys. Res. Lett.* **2005**, *32*.

- (5) Kawamura, K.; Ng, L. L.; Kaplan, I. R. *Environ. Sci. Technol.* **1985**, *19*, 1082.
- (6) Kesselmeier, J.; Staudt, M. *J. Atmos. Chem.* **1999**, *33*, 23.
- (7) Ito, A.; Sillman, S.; Penner, J. E. *J. Geophys. Res.* **2007**, *112*.
- (8) von Kuhlmann, R.; Lawrence, M.; Crutzen, P.; Rasch, P. *J. Geophys. Res.* **2003**, *108*, 4294.
- (9) Orlando, J. J.; Tyndall, G. S. *J. Photochem. Photobiol. A* **2003**, *157*, 161.
- (10) Dickerson, R. R.; Huffman, G. J.; Luke, W. T.; Nunnermacker, L. J.; Pickering, K. E.; Leslie, A. C. D.; Lindsey, C. G.; Slinn, W. G. N.; Kelly, T. J.; Daum, P. H.; Delany, A. C.; Greenberg, J. P.; Zimmerman, P. R.; Boatman, J. F.; Ray, J. D.; Stedman, D. H. *Science* **1987**, *235*, 460.
- (11) Thompson, A. M.; Tao, W. K.; Pickering, K. E.; Scala, J. R.; Simpson, J. B. *Am. Meteorol. Soc.* **1997**, *78*, 1043.
- (12) Jost, H.-J.; Drdla, K.; Stohl, A.; Pfister, L.; Loewenstein, M.; Lopez, J. P.; Hudson, P. K.; Murphy, D. M.; Cziczko, D. J.; Fromm, M.; Bui, T. P.; Dean-Day, J.; Gerbig, C.; Mahoney, M. J.; Richard, E. C.; Spichtinger, N.; Pittman, J. V.; Weinstock, E. M.; Wilson, J. C.; Xueref, I. *Geophys. Res. Lett.* **2004**, *31*, L11101.
- (13) Fischer, H.; de Reus, M.; Traub, M.; Williams, J.; Lelieveld, J.; de Gouw, J.; Warneke, C.; Schlager, H.; Minikin, A.; Scheele, R.; Siegmund, P. *Atmos. Chem. Phys.* **2003**, *3*, 739.
- (14) Singh, H.; Chen, Y.; Tabazadeh, A.; Fukui, Y.; Bey, I.; Yantosca, R.; Jacob, D.; Arnold, F.; Wohlfrom, K.; Atlas, E.; Flocke, F.; Blake, D.; Blake, N.; Heikes, B.; Snow, J.; Talbot, R.; Gregory, G.; Sachse, G.; Vay, S.; Kondo, Y. *J. Geophys. Res.* **2000**, *105*, 3795.
- (15) Butkovskaya, N. I.; Kukui, A.; Pouvesle, N.; Le Bras, G. *J. Phys. Chem. A* **2004**, *108*, 7021.
- (16) Wallington, T. J.; Schneider, W. F.; Worsnop, D. R.; Nielsen, O. J.; Sehested, J.; Debruyne, W. J.; Shorter, J. A. *Environ. Sci. Technol.* **1994**, *28*, A320.
- (17) Ellis, D. A.; Martin, J. W.; De Silva, A. O.; Mabury, S. A.; Hurley, M. D.; Andersen, M. P. S.; Wallington, T. J. *Environ. Sci. Technol.* **2004**, *38*, 3316.
- (18) Bowden, D. J.; Clegg, S. L.; Brimblecombe, P. *Chemosphere* **1996**, *32*, 405.
- (19) Mögelberg, T. E.; Nielson, O. J.; Sehested, J.; Wallington, T. J.; Hurley, M. D. *Chem. Phys. Lett.* **1994**, *226*, 171.
- (20) Golden, D. M.; Spokes, G. N.; Benson, S. W. *Angew. Chem., Int. Ed.* **1973**, *12*, 534.
- (21) Carslaw, K. S.; Clegg, S. L.; Brimblecombe, P. *J. Phys. Chem.* **1995**, *99*, 11557.
- (22) Massucci, M.; Clegg, S. L.; Brimblecombe, P. *J. Phys. Chem. A* **1999**, *103*, 4209.
- (23) Brimblecombe, P.; Clegg, S. L.; Wexler, A. S. *Aerosol Inorganics Model*; <http://www.aim.env.uea.ac.uk/aim/aim.php>.
- (24) Michelsen, R. R.; Staton, S. J. R.; Iraci, L. T. *J. Phys. Chem. A* **2006**, *110*, 6711.
- (25) Finlayson-Pitts, B. J.; Pitts, J. N., Jr. *Chemistry of the Upper and Lower Atmosphere*; Academic Press: San Diego, 2000.
- (26) Reid, R. C.; Prausnitz, J. M.; Poling, B. E. *The Properties of Gases and Liquids*, 4th ed.; McGraw-Hill: New York, 1987.
- (27) Williams, L. R.; Long, F. S. *J. Phys. Chem.* **1995**, *99*, 3748.
- (28) Dankwerts, P. V. *Gas-Liquid Reactions*; McGraw-Hill Book Co.: New York, 1970.
- (29) Johnson, B. J.; Betterton, E. A.; Craig, D. J. *Atmos. Chem.* **1996**, *24*, 113.
- (30) Henne, A. L.; Fox, C. J. *J. Am. Chem. Soc.* **1951**, *73*, 2323.
- (31) Klassen, J. K.; Hu, Z.; Williams, L. R. *J. Geophys. Res.* **1998**, *103*, 16197.
- (32) Williams, L. R.; Golden, D. M. *Geophys. Res. Lett.* **1993**, *20*, 2227.
- (33) Williams, L. R.; Golden, D. M.; Huestis, D. L. *J. Geophys. Res.* **1995**, *100*, 7329.
- (34) Iraci, L. T.; Essin, A. M.; Golden, D. M. *J. Phys. Chem. A* **2002**, *106*, 4054.
- (35) Duncan, J. L.; Schindler, L. R.; Roberts, J. T. *J. Phys. Chem. B* **1999**, *103*, 7247.
- (36) Klassen, J. K.; Lynton, J.; Golden, D. M.; Williams, L. R. *J. Geophys. Res.* **1999**, *104*, 26355.

- (37) Hogeveen, H.; Bickel, A. F.; Hilbers, C. W.; Mackor, E. L.; Maclean, C. *Chem. Commun.* **1966**, 898.
- (38) Goldfarb, A. R.; Mele, A.; Gutstein, N. *J. Am. Chem. Soc.* **1955**, 77, 6194.
- (39) Liler, M. *J. Chem. Soc.* **1965**, 4300.
- (40) Cox, R. A. Excess acidities. In *Advances in Physical Organic Chemistry*; Academic Press Ltd.: London, 2000; Vol. 35, p 1.
- (41) Lee, D. G.; Sadar, M. H. *Can. J. Chem.* **1976**, 54, 3464.
- (42) Liler, M. *Reaction Mechanisms in Sulphuric Acid and Other Strong Acid Solutions*; Academic Press: London, New York, 1971.
- (43) Bagno, A.; Lucchini, V.; Scorrano, G. *J. Phys. Chem.* **1991**, 95, 345.
- (44) Michelsen, R. R.; Ashbourn, S. F. M.; Iraci, L. T. *J. Geophys. Res.* **2004**, 109, D23205.
- (45) Myhre, C. E. L.; Christensen, D. H.; Nicolaisen, F. M.; Nielsen, C. J. *J. Phys. Chem. A* **2003**, 107, 1979.
- (46) Wilson, B.; Georgiadis, R.; Bartmess, J. E. *J. Am. Chem. Soc.* **1991**, 113, 1762.
- (47) Colominas, C.; Teixido, J.; Cemeli, J.; Luque, F. J.; Orozco, M. *J. Phys. Chem. B* **1998**, 102, 2269.
- (48) Christian, S. D.; Stevens, T. L. *J. Phys. Chem.* **1972**, 76, 2039.
- (49) Chocholousova, J.; Vacek, J.; Hobza, P. *J. Phys. Chem. A* **2003**, 107, 3086.
- (50) Williams, L. R.; Manion, J. A.; Golden, D. M.; Tolbert, M. A. *J. Appl. Meteorol.* **1994**, 33, 785.
- (51) Talbot, R. W.; Dibb, J. E.; Lefer, B. L.; Scheuer, E. M.; Bradshaw, J. D.; Sandholm, S. T.; Smyth, S.; Blake, D. R.; Blake, N. J.; Sachse, G. W.; Collins, J. E.; Gregory, G. L. *J. Geophys. Res.* **1997**, 102, 28303.
- (52) Reiner, T.; Mohler, O.; Arnold, F. *J. Geophys. Res.* **1999**, 104, 13943.
- (53) Jacob, D. J.; Heikes, B. G.; Fan, S. M.; Logan, J. A.; Mauzerall, D. L.; Bradshaw, J. D.; Singh, H. B.; Gregory, G. L.; Talbot, R. W.; Blake, D. R.; Sachse, G. W. *J. Geophys. Res.* **1996**, 101, 24235.